Ab Initio Molecular Dynamics Investigation of the Formyl Cation in the Superacid SbF 5 /HF

ARTICLE *in* THE JOURNAL OF PHYSICAL CHEMISTRY B · AUGUST 2001

Impact Factor: 3.3 · DOI: 10.1021/jp0106855

2 AUTHORS, INCLUDING:

Simone Raugei

Pacific Northwest National Laboratory

96 PUBLICATIONS **1,742** CITATIONS

SEE PROFILE

Ab Initio Molecular Dynamics Investigation of the Formyl Cation in the Superacid SbF_5/HF

Simone Raugei* and Michael L. Klein

Center for Molecular Modeling and Department of Chemistry, University of Pennsylvania, Philadelphia, Pennsylvania 19104-6323

Received: February 21, 2001; In Final Form: April 19, 2001

The formyl cation (HCO^+) is an intermediate involved in electrophilic formylation reactions of aromatic compounds. We have employed ab initio molecular dynamics simulation to investigate free energy profiles along several possible reaction paths for CO in the SbF_5/HF superacid solution for different concentrations of SbF_5. The formation of the HCO^+ cation is optimally favored in the 1:1 SbF_5/HF solution. However, no evidence has been found for the presence of either the isoformyl cation, COH^+, or the protoformyl dication, $HCOH^{2+}$. A novel mechanism for the experimentally observed fast proton exchange in the system CO in 1:1 SbF_5/HF is proposed.

I. Introduction

One of the major achievements of modern chemistry is the development of spectroscopic methods for direct characterization of short-lived reaction intermediates.[1] The observation of positively charged carbocation intermediates under long-lived stable conditions in superacid media has opened new horizons for synthetic and theoretical chemistry.[2,3] "Superacids" are stronger than conventional strong mineral Brønsted acids such as sulfuric acid or Lewis acids such as aluminum trichloride. The solution of antimony pentafluoride (SbF_5) in liquid hydrogen fluoride (HF) is one of the strongest known superacids, being about 10^{18} times stronger than 100% sulfuric acid.[2] It can protonate extremely weak bases such as alkanes,[2] and it has been used for a large variety of catalytic and synthetic applications including industrial scale processes involving hydrocarbon transformations such as cracking, isomerization, and alkylation.[4] Recently, the elusive formyl cation (HCO^+) has been characterized in a superacid medium.[5] The formyl cation is an intermediate involved in electrophilic formylation reactions of aromatic compounds via the Gatterman−Koch reactions.[2,3] It has been observed as a reasonably abundant species in interstellar molecular clouds,[6,7] and it has been suggested as a primary ionic product formed in hydrocarbon combustion.[8] Although the formyl cation may be easily generated in the gas phase by a variety of methods,[9] it has eluded direct observation in the condensed phase. Attempts to synthesize the formyl cation via direct protonation of CO in a superacid such as FSO_3H/SbF_5 failed. Even at low temperature and under low CO pressure (<10 atm), which should shift the protonation equilibrium

$$H^+ + CO \rightleftharpoons HCO^+$$

to the right, CO was observed in a nonprotonated state.[10] Attempts to try to abstract F^- from formyl fluoride, H(F)C═O, with SbF_5[10] or dehydrate formic acid[10,11] also proved futile. However recently, de Rege et al.[5] reported the observation of HCO^+ in SbF_5/HF (1:1) under CO pressure up to 85 atm by ^{13}C NMR and infrared spectroscopy. At low pressure and room temperature the formyl cation, HCO^+, gives rise to a single peak at 145 ppm in the proton-coupled ^{13}C NMR spectrum observed along with a doublet of doublets at 179 ppm attributed to the formyl fluoride oxygen complexed to antimony pentafluoride, $H(F)CO{\rightarrow}SbF_5$. On increasing the temperature, the HCO^+ signal at 145 ppm moved to 139.5 ppm, and its intensity relative to that of $H(F)CO{\rightarrow}SbF_5$ increases from 0.43 to 0.75 as the CO pressure increased from 3 to 85 atm, respectively. In these NMR experiments no $^{13}C-^1H$ scalar coupling was observed, indicating a fast proton exchange with the solution. This hypothesis was supported by the proton NMR spectrum where no separate signal from the HCO^+ cation was observed. The explanation of de Rege et al.[5] for the proton exchange invoked the formation of the protoformyl dication ($HCOH^{2+}$) and isoformyl cation (COH^+):

$$\begin{array}{ccc} CO & \overset{H^+}{\rightleftharpoons} & COH^+ \\ \downarrow\uparrow H^+ & & \downarrow\uparrow H^+ \\ HCO^+ & \overset{H^+}{\rightleftharpoons} & HCOH^{2+} \end{array} \qquad (1)$$

This proposal has been referred as speculative[12] since in superacid media a rapidly equilibrating protosolvated ion

$$H{-}C{\equiv}O^+{\cdots}HA \overset{H^+}{\rightleftharpoons} COH^+ \rightleftharpoons CO + H^+ \qquad (2)$$

could also be involved, as suggested many years ago by Olah et al.[11] Moreover, it is still unclear why the dilution of SbF_5/HF with SO_2ClF (1:4) or HF (1:3) resulted in the disappearance of the NMR signal assigned to the formyl cation[5] as previously reported.[10,11,13] Interestingly, the acidity of HSO_3/SbF_5 was not sufficient to generate HCO^+ or H(F)CO either free or complexed to SbF_5.

To shed light on the chemistry of CO in superacid media, we have performed an ab initio Car−Parrinello (CP)[14] study of the reactivity of CO in SbF_5/HF solutions. We have investigated possible HCO^+ formation in (a) the 1:1 (50%) solution, (b) a dilute SbF_5/HF solution (4% SbF_5), and (c) liquid HF with an excess proton. Our group has already studied superacid media, such as the BF_3/HF[15] and the SbF_5/HF (4% SbF_5) systems[16], and an excess proton in HF using ab initio simulations.[17] The

* Corresponding author. E-mail: raugei@cmm.chem.upenn.edu.

10.1021/jp0106855 CCC: $20.00
Published on Web 08/04/2001

TABLE 1: Gas-Phase Reaction ΔE_0 and Activation Energies $\Delta E^{\ddagger}$ (in kJ mol^{-1}) of Several Processes Involved in the Chemistry of CO in SbF_5/HF[a]

	ΔE_0				$\Delta E^{\ddagger}$		
reaction	HCTH	BLYP	MP2	expt	HCTH	BLYP	MP2
$CO + H^+ \rightarrow HCO^+$	−624.4	−765.7	−624.7	−593.7[b]	0.0	0.0	0.0
$CO + H^+ \rightarrow COH^+$	−453.7	−436.1	−431.3	−432.9[c]	0.0	0.0	0.0
$HCO^+ + H^+ \rightarrow HCOH_2^+$	+274.7	+279.4	+295.3		449.6	287.0	518.3
$COH^+ + H^+ \rightarrow HCOH_2^+$	+107.3	+110.7	+101.9		315.1	216.4	324.9
$H(F)CO + SbF_5 \rightarrow H(F)CO \rightarrow SbF_5$	−31.0				0.0		
$H(CO)F + SbF_5 \rightarrow H(CO)F \rightarrow SbF_5$	−2.2				0.0		

[a] The HCTH and BLYP calculations utilized a PW basis set (70 Ry cutoff), whereas the MP2 results are for an AUG-cc-pVTZ Gaussian basis set. [b] Proton affinity at 298 K from: Woods, R. C.; Dixon, T. A;. Saykally, R. J.; Szanto, P. G. *Phys. Rev. Lett.* **1975**, *35*, 1269. [c] Heat of formation at 298 K from: Lias, G.; Bartmess, J. E.; Liebman, J. F.; Holmes, J. L.; Levin, R. D.; Mallard, W. G. *J. Phys. Chem. Ref. Data* **1988**, *17*(S1), 1−872.

results obtained show clearly how the CP technique is capable of revealing microscopic details of reaction mechanisms that are relevant for a deeper understanding of the experimental results. In the present study we will investigate why (1) the formation of formyl cation is possible only for high SbF_5 concentration and (2) the proposed mechanisms for the fast proton exchange involving the protoformyl dication and isoformyl cation or the protosolvation of the formyl cation are not likely. Indeed, anticipating our results, we suggest the proton exchange could be due to a proton transportation role of the newly formed formyl cation.

The paper is organized as follows. In section II, we will give the computational details of our simulations. In section III we will analyze the structure of the superacid solution SbF_5/HF (1:1). Then, in section IV the results of our study on the chemical reactivity of CO in SbF_5/HF will be given and analyzed. The article ends with conclusions.

II. Computational Details

A. Electronic Structure. We have performed first principles molecular dynamics (MD) simulations within the so-called CP scheme[14] (CPMD), which employs density functional theory (DFT) for the electronic structure calculations. Among the ab initio techniques, DFT is now a well-established predictive tool for its computational speed and its ability to give geometries, frequencies, and heats of reaction comparable to those obtained by second-order Møller−Plesset perturbation theory (MP2).[18−21] The CPMD DFT scheme is particularly suited to condensed-phase simulations employed here. Indeed, the CPMD method has already been used to study chemical reactions,[22−38] and it has been shown to be an excellent tool to fully understand the chemical kinetics at a microscopic level. However, the majority of the studies of chemical reactivity carried out so far using DFT seem to indicate that the reaction barrier heights are underestimated (see, for example, refs 39 and 40). This has been reported[22,32,33] to be the case for the very popular Becke, Lee, Yang, and Parr (BLYP) exchange and correlation functional, which uses the Becke exchange[41] (B) and the Lee et al. correlation energy[42] (LYP), or its improved modification B3LYP,[43,44] on the basis of a comparison with both MP2 calculations and experimental results. To apply the DFT method to the studies of chemical reaction mechanisms, the question of the accuracy of the calculated barrier heights is of primary importance.

In the present study we have used the new empirical exchange-correlation functional proposed by Hamprecht et al.,[45,46] named HCTH. This functional has been successfully used to evaluate the geometry and the energy along the reaction pathway of simple S_N2 reactions,[23,47,40] obtaining an improvement in the energy profile with respect to the BLYP functional, and it has been demonstrated to be more satisfactory in describing the hydrogen bond in liquid water than BLYP.[46]

The present DFT calculations utilized Troullier−Martins pseudopotentials[48] to describe the core of all atoms except for hydrogen, for which a von Barth−Car analytical pseudopential[49] has been used. The Kleiman−Bylander decomposition[50] was used for F, C, and O atoms, while for Sb the Gauss−Hermite[51] scheme was employed. The electronic wave functions were expanded in a plane wave (PW) basis set up to the energy cutoff of 70 Ry. With this choice the molecular geometries converged to within about 0.3%.

The reliability of the HCTH functional for the present study has been tested by performing gas-phase calculations on the main species that are supposed to be involved in the formation of formyl cation in the condensed phase. We have compared the HCTH results with BLYP functional calculations and MP2/AUG-cc-pVTZ level of theory. All the DFT/PW test calculations were done using the CPMD program[52] and the MP2 calculations used the Gaussian 98 package.[53] The PW calculations were performed in a cubic box with dimensions ranging between 11 and 14 Å, depending on the size of the system, and the usual technique to consider the system isolated was employed.[54,55] The results obtained are summarized in Table 1. Our MP2 calculations agree well with the MP2/6-31G*/G2 results reported previously by Hartz et al.[56] At every level of theory we have found no barrier for the formation of HCO^+ and COH^+ cations. The BLYP functional overestimates the formation energy for the HCO^+ cation with respect to the HCTH functional and MP2 calculations. For both HTCH and MP2 level calculations, the formation of the $HCOH^{2+}$ dication from HCO^+ or COH^+ presents a prohibitively high energy barrier. The agreement between HCTH and MP2 is fairly good for both the reaction and the activation energies. The BLYP functional predicts a value for the formation energy of the dication in agreement with the other methods but gives a much lower barrier for its decomposition, confirming the general trend reported in the literature.

To conclude, as can be seen from Table 2, the geometries of molecules computed at the HCTH level are in agreement with the MP2 and experiment, even though HCTH has a tendency to overestimate the C−H bond length. Overall, at the HCTH level, we have fairly good agreement with experiment and MP2 calculations.

B. The Simulation System. We have studied CO reactivity in SbF_5/HF at 300 K for three limiting cases, namely the high (50%) and the low (4%) SbF_5 concentration solutions, and in liquid HF with an excess proton (infinite dilution). The starting configurations for the reaction in the HF/H^+ and the 4% SbF_5/

TABLE 2: Computed Bond Distances (*d*) in Angstroms and Bond Angles (∠) in Degrees of Selected Molecules[a]

molecule	parameter	HCTH	BLYP	MP2	expt
Sb_2	*d*(Sb−Sb)	2.491	2.478		2.49[b]
HF	*d*(H−F)	0.930	0.932	0.917	0.92[c]
CO	*d*(C−O)	1.136	1.136	1.139	1.128[d]
HCO^+	*d*(H−C)	1.100	1.096	1.091	1.097[e]
	d(C−O)	1.112	1.113	1.119	1.105[e]
	∠(H−C−O)	180.0	180.0	180.0	180.0[e]
COH^+	*d*(C−O)	1.168	1.160	1.159	1.157[f]
	d(O−H)	1.007	1.007	0.995	0.975[f]
	∠(H−C−O)	180.0	180.0	180.0	180.0[f]
$HCOH_2^+$	*d*(H−C)	1.154	1.150	1.140	
	d(C−O)	1.124	1.127	1.123	
	d(O−H)	1.071	1.080	1.072	
	∠(H−C−O)	180.0	180.0	180.0	
	∠(C−O−H)	180.0	180.0	180.0	
H(F)CO	*d*(H−C)	1.096	1.096	1.094	
	d(F−C)	1.364	1.386	1.351	
	d(C−O)	1.185	1.189	1.185	
	∠(H−C−O)	128.1	129.1	128.2	
H(F)CO → SbF_5	*d*(H−C)	1.100	1.097		
	d(F−C)	1.321	1.321		
	d(C−O)	1.205	1.206		
	∠(H−C−F)	113.1	113.0		
	$d(H-F'_a)$	2.659	2.581		
	d(O−Sb)	2.341	2.350		
	$d(Sb-F_e)$	1.847	1.831		
	$d(Sb-F'_e)$	1.864	1.857		
	$d(Sb-F_a)$	1.834	1.830		
SbF_6	*d*(Sb−F)	1.878	1.918		1.87[g]

[a] The HCTH and BLYP calculations were performed with a PW basis set (see text), whereas the MP2 calculations use a AUG-cc-pTVZ Gaussian basis set. [b] Latajka, Z.; Boutellier, Y. *J. Chem. Phys.* **1994**, *101*, 9793. [c] Mootz, D.; Bartmann, K. Z. *Naturforsch.* **1991**, *46b*, 1659. [d] Amano, T.; et al. *J. Chem. Phys.* **1983**, *79*, 3595. [e] Wood, R. C.; et al. *Philos. Trans. R. Soc., A* **1984**, *324*, 141. [f] Berry, R. J.; Harmony, M. D. *J. Mol. Spectros.* **1988**, *128*, 176. [g] The average bond length taken from the $H_5O_2^+SbF_6^-$ crystal structure. Minkwitz, R.; Schneider, S.; Kornath, A. *Inorg. Chem.* **1998**, *37*, 4662.

HF solutions were obtained from our previous studies on the HF/H^+ and the SbF_5/HF solutions.[16,17] The former system consists of 54 HF molecules and an H^+ proton contained in a cubic cell of 12.1711 Å side. The latter has 25 HF molecules and one SbF_5 molecule contained in a cubic cell of 9.8797 Å side. The starting configuration for the high concentration solution was obtained from several ab initio annealing simulations on configurations generated by putting at random six SbF_5 and six HF units in a cubic cell of 10.8839 Å side. The volume was chosen on the basis of the experimental densities of liquid SbF_5 and HF under ambient conditions. The small numbers of atoms was dictated by the large computational effort needed to study a bigger system. The random starting configurations converged to a similar equilibrium configuration. The structural properties of the 50% SbF_5/HF solution will be discussed in the next section. The CO/SbF_5/HF systems were studied by replacing at random an HF molecule with carbon monoxide or inserting a CO molecule in a well-equilibrated SbF_5/HF solution, as described in the following sections, and reequilibrating the system at 300 K for a few picoseconds.

We would like to point out that the size of the systems we have studied can impose limitations on the range of phenomena that can be described. Nevertheless, the effects of the boundary on the basic chemical reactions are not expected to qualitatively change the results. In fact, as it will be shown in the following, the key processes that take place are driven by the local environment around the CO molecule.

C. Constrained Molecular Dynamics. Although in the gas phase there is no energy barrier for HCO^+ cation formation, in the condensed phase bond breaking and formation processes involve the crossing of a relatively large activation barrier. For this reason in the present study we adopted the method of constrained molecular dynamics called the *Blue Moon Ensemble*.[57,58] This technique allows us to sample a chosen reaction path with the desired accuracy and to obtain the free energy profile along it. The reaction coordinate was chosen to be the distance $\zeta = |R_H - R_X|$ between a randomly chosen H atom and the C or O atom distance (X = C or O) as discussed below. The crucial technical details about the treatment of the constrained reaction coordinate are given in the paper by Sprik and Ciccotti.[57] We will limit the discussion to the formula strictly necessary to the present discussion. Briefly, the holonomic constraint $\zeta = \zeta_0$ is included into the Car−Parrinello Lagrangian

$$L = L^{CP} + \lambda[\zeta(|R_H - R_X|) - \zeta_0]$$

where λ is the Lagrange multiplier associated with the chosen constraint and corresponds to the *mean force*. Exploring the constrained phase space allows one to compute the mean constrained force, and from this the change in free energy can be computed according to the *Blue Moon* method[57,58]

$$\Delta F = -\int_A^B d\zeta_0 \langle\lambda(\zeta_0)\rangle$$

where *A* and *B* are the initial and final values of the reaction coordinate ζ_0. In our convention, a negative value of the mean force indicates that H is pulled in the direction of X (C or O), and a positive value indicates that H and X tend to separate. A zero value of the mean force means that the system is at the equilibrium (stationary point) or that there is no interaction between X and H. We observe in passing that the free energy as computed in the present scheme fully includes all the anharmonicity of the potential energy surface of the system and finite temperature effects. The statistical uncertainty on the free energy estimation is of the order of k_BT. This is the typical accuracy allowed by ab initio simulations.[24,25,37,59,60]

The equations of motion have been integrated with a time step ranging between 0.09 and 0.17 fs using a fictitious electronic mass[14] ranging between 800 and 1000 au, depending on the system. The temperature was controlled by coupling the system with a Nosé−Hoover chain of thermostats.[61] For each point of the reaction coordinate we studied, the system was equilibrated for about 2 ps and then trajectories were collected for about 4 ps. Further computational details will be given in the following sections whenever they are deemed necessary.

III. The SbF_5/HF 1:1 Solution

Before discussing the reactivity of CO in the superacid, we will briefly report on the structure of the 50% SbF_5/HF solution as inferred from the CPMD simulations. As already been mentioned in section II, we have performed several annealing simulations of a randomly obtained configuration of SbF_5 and HF units. Each starting random configuration (out of a total of four) evolved spontaneously with a barrierless, diffusion limited reaction, giving in a few picoseconds Sb atoms octahedrally coordinated with F atoms in agreement with what was observed in the previous study of 4% SbF_5/HF solution.[17] At this point, the Sb mass was reduced to 40 amu for about 2 ps in order to speed up the process and the temperature was maintained at about 300 K by uniformly scaling the velocities. Next, the structure was relaxed with a simulated annealing-like procedure bringing the temperature first to 600 K and then cooling to 300 K. The system was then equilibrated for about 3 ps using a

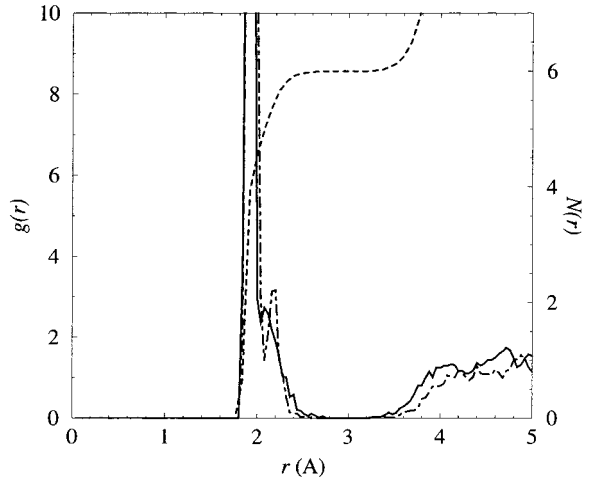

Figure 1. Radial distribution function $g(r)$ for Sb−F pair in the 50% SbF_5/HF (solid line) and the 4% (dashed−dotted line) solutions. The dashed line indicates the number of F atoms $N(r)$ located at distance r from a Sb atom in the 50% solution.

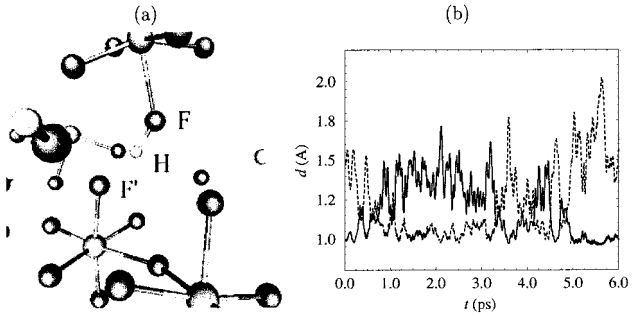

Figure 2. Proton exchange between $Sb_2F_{11}^-$ and SbF_6^- units in the 50% SbF_5/HF solution. (a) Snapshot of a configuration. (b) Time evolution of the F−H (solid) and F′−H (dashed) distances indicating proton exchange between these two different units.

Nosé−Hoover chain of thermostats to control the temperature, after which a trajectory in the phase space was sampled for about 6 ps.

The octahedral coordination of the Sb atoms is evident from the radial distribution function $g(r)$ of the Sb−F pairs and the coordination number $N(r)$ of the Sb atoms reported in Figure 1 along with the $g(r)$ of the 4% solution. In 4% SbF_5/HF,[17] it was found that after an initial period in which an HF molecule is coordinated to SbF_5 giving SbF_5–FH, a contact ion pair SbF_6^-:H_2F^+ is formed. In the 50% solution the SbF_5 units have the tendency to form $Sb_nF_{5n+1}^-$ anions with $n = 1$ and 2, i.e., charged monomers and dimers (see Figure 2a). In the case of dimers only one HF molecule is coordinated to a Sb_2F_{10} unit. Hence, not all of the HF molecules are ligands and these remaining molecules can give rise to H_2F^+ ions. It can also happen that one of the HF molecules coordinated to Sb does not have an HF nearby to which an H^+ can be transferred. Thus, it will form Sb_nF_{5n} $-F^{\dagger}H$ with a very polar $F^{\dagger}-H$ bond. In the following we will indicate with F† a F atom directly bonded to Sb. The proton of this $F^{\dagger}-H$ bond can be freely exchanged between two adjacent $Sb_nF_{5n+1}^-$ units as can be seen from Figure 2b. For this reason, it is perhaps appropriate to indicate the Sb_nF_{5n} $-F\dagger H$ unit as $Sb_nF_{5n+1}^-$:H^+.

The H_2F^+ cations are associated in contact ion pairs $Sb_nF_{5n+1}^-$:H_2F^+ with $n = 1$ and 2, where H_2F^+ is directly bonded to one of the $Sb_nF_{5n+1}^-$ anions via a $F^{\dagger}\cdots H$ hydrogen bond. There are few free HF molecules in the concentrated solution. Hence, the contact ion pair cannot evolve into a fully separated ion pair as found in the dilute solution. Instead, H_2F^+ cations stay close to the $Sb_nF_{5n+1}^-$ anions being separated at most by one HF molecule. H_2F^+ cations shared between two $Sb_nF_{5n+1}^-$ were also observed.

Solutions of SbF_5 in HF are known to involve complex equilibria between various $Sb_nF_{5n+1}^-$ anions.[62] Gillespie and Moss[63] demonstrated the presence of $Sb_2F_{11}^-$ by ^{19}F NMR spectroscopy in 20% SbF_5−80% HF and hypothesized a progressive polymerization as the concentration is increased. Of course, in our simulations, size effects will impose limitation in describing structural features of the high concentration solution, such as the extent of the oligomerization as $Sb_nF_{5n+1}^-$ and, perhaps, also the maximum length of the HF chains. However, it is reasonable to assume that the local structure around an SbF_6 unit is, at least qualitatively, well reproduced along with the behavior of the ion pairs. Our explanation of the chemistry of CO in this superacid system is based on these assumptions. To conclude, we stress that it is the presence of almost free protons which makes the 50% solution a very strong superacid medium.

IV. Reactivity of CO in SbF_5/HF

A. Formyl Cation Formation. In principle, the protonation of CO in the SbF_5/HF superacid might be carried out by (i) the proton directly bonded to the $F^{\dagger}$ atom (see previous section, and Figure 3a,b), (ii) the pendant proton of an H_2F^+ cation of a $Sb_nF_{5n+1}^-$:H_2F^+ contact ion pair (Figure 3c), or, in the case of a dilute solution, (iii) an H_2F^+ cation well separated from the $Sb_nF_{5n+1}^-$ anion in the bulk of the HF solution (Figure 3d). We have investigated routes (i) and (ii) in both the 50% and 4% SbF_5/HF solutions and route (iii) in the HF solution with an excess proton. To study the energy profile along these reaction paths in the 50% solution, we have added a CO molecule near a proton chosen at random and increased the system volume to allow for the van der Waals radius of CO. In the case of the 4% solution and for HF with an excess proton, we have simply replaced by CO an HF molecule, not belonging to the HF chain involved in the proton jump diffusion process, near the selected proton. In both cases, the system was reequilibrated for few picoseconds, keeping the H···C distance fixed at about 1.6 Å.

In the high concentration solution, route (i) for the protonation is very likely because there is an high probability of having $Sb_nF_{5n+1}^-$:H^+ (or $Sb_nF_{5n+1}^-$:H_2F^+). The free energy profile for this kind of proton transfer is reported in parts a and b of Figure 4 for the 50% and the 4% solutions, respectively. As evident from the figure, the proton is easily transferred, and when the distance H···C goes below about 1.17 Å, the HCO^+ cation spontaneously separates. The formyl cation formation requires the crossing of a very low free energy barrier: about 4 and 10 kJ mol^{-1} for the 50% and 4% solutions, respectively. The higher value obtained for the 4% solution is related to the energy required for the breaking of the H···F hydrogen bond between the transferred proton and the HF chain.

The situation for proton transfer in route (ii) is completely different. The energy profile calculated for the 4% solution is reported in Figure 4c. The curve does not show any minimum, and no HCO^+ cation formation was observed in the simulations. It was not possible to go below $\zeta = 1.10$ Å because the sampling became increasingly difficult, owing to the increase in strength of the constraint force. Also, in the 50% solution, route (ii) did not lead to the HCO^+ cation.

For route (iii) it was impossible to study the energy profile for the proton transfer. In this case the mean force rapidly

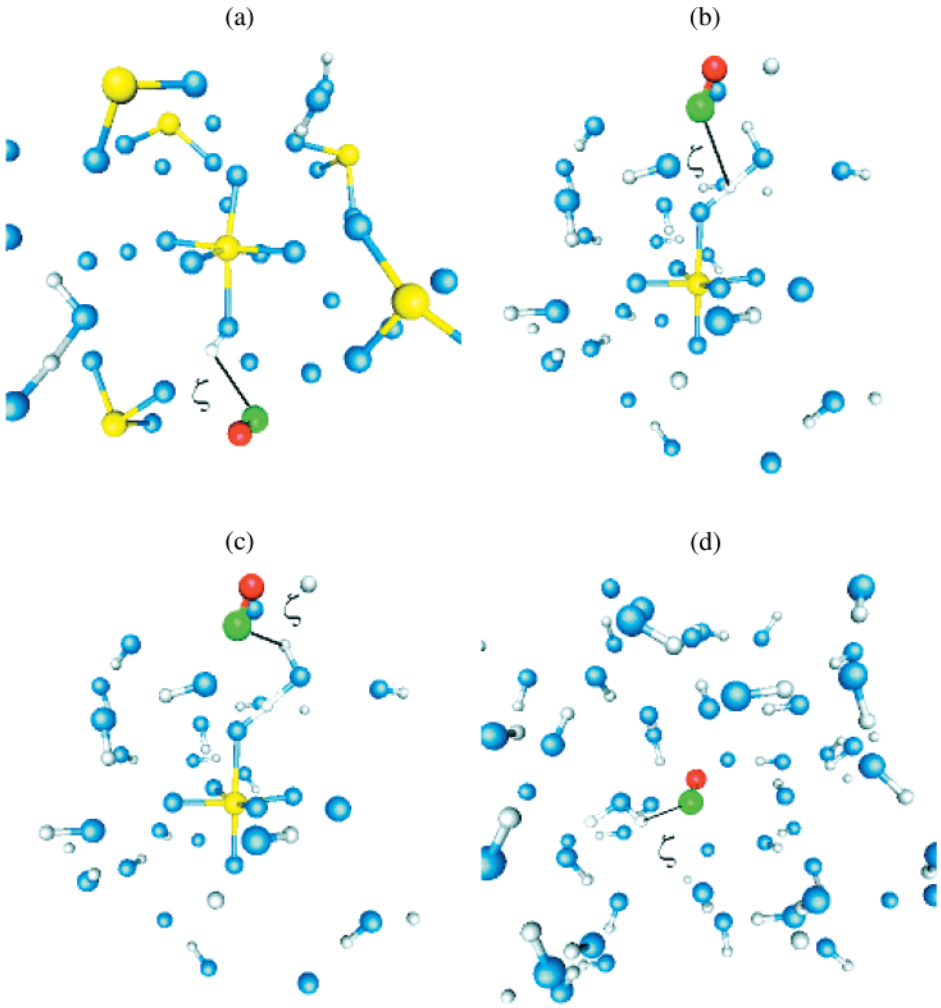

Figure 3. Four different proton-transfer paths ζ examined: (a) and (b) proton directly bonded to an SbF_6 unit in the 50% and 4% solutions, respectively; (c) pendant proton of an H_2F^+ cation belonging to the contact ion pair SbF_6^-:H_2F^+ in the 4% solution; (d) proton of a H_2F^+ cation in bulk HF solution. Green, carbon; red, oxygen; yellow, antimony; blue, fluorine; gray, hydrogen.

increases below $\zeta = 1.6$ Å. This indicates that the H atom of the H_2F^+ ion is strongly pulled in the direction of F. For a distance below 1.3 Å the system spontaneously evolved giving H(F)CO:

$$CO + H_2F^+\cdot(HF)_m^{chain} \rightarrow H(F)CO + H_2F^+\cdot(HF)_{m-1}^{chain}$$

However, the free energy required for this reaction is very large, as the value of the mean force indicated. It was not possible to estimate the free energy profile. In fact, due to the high value of the mean force along the reaction coordinate before H(F)CO molecule formation, it can happen that the H_2F^+ cation breaks transferring a proton to the HF chain (restoring in this way the H_2F^+ cation). This behavior could be the result of some inadequacy of the selected reaction coordinate. A simple linear reaction path can give a poor description of the process when a strongly polar solvent is present because of the complexity of the components of the reaction coordinate (corresponding to solvent reorganization), which are usually not known in advance.[64] On the other hand, when the simulation was started from HCO^+ in liquid HF, the formyl cation promptly donated its proton to the solvent. This indicates that the barrier for the reverse reaction is almost negligible, and this makes the product highly unstable as will be evident from the ensuing discussion.

We have also studied the possibility of CO protonation on the oxygen side. The results obtained for the 50% SbF_5/HF solution are reported in Figure 4d. As for route (ii), the free energy profile is always repulsive and the process does not seem possible. This would rule out the possibility of having COH^+ formed in this superacid via direct protonation.

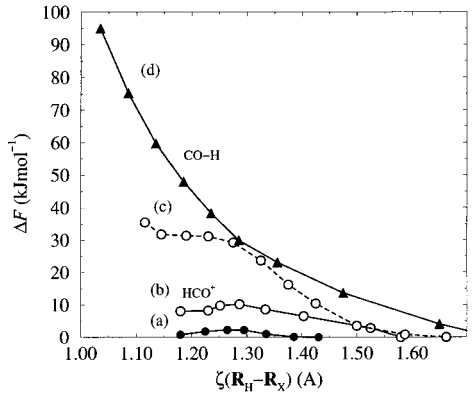

Figure 4. Free energy profile ΔF along the reaction cordinate $\zeta = |\mathbf{R}_H - \mathbf{R}_X|$ (see text): (a) and (b) proton transfer from the HF molecule directly coordinated to an Sb atom in the 50% and 4% solutions, respectively (X = C); (c) proton transfer from H_2F^+ of the SbF_6^-:H_2F^+ contact ion pair (X = C); (d) as in (a) but with the proton transferred to the O atom (X = O).

Before discussing the possible reactive channels of the HCO^+ cation and the proposed mechanism for the experimentally observed fast proton exchange, we will analyze the origin of

TABLE 3: Calculated Protonation Energy ΔE_0 and Proton Affinity A_n (both in kJ mol^{-1}) of H_nF_n Chains and for Carbon Monoxide[a]

	HCTH		MP2	
n	ΔE_0	A_n	ΔE_0	A_n
1	−509.7	491.9	−505.6	493.9
2	−636.8	617.2	−621.3	600.0
3	−684.8	665.7	−687.7	668.9
4			−729.3	
5			−746.2	
CO	−624.4	600.9	−624.7	606.3
CO	−453.7	437.9	−431.7	414.7

[a] C′O and CO′ indicate C-side and O-side protonation, respectively. The HCTH calculations utilized a PW basis set (70 Ry cutoff), whereas the MP2 results are for a 6-311++G(d,p) Gaussian basis set (geometries optimized with a AUG-cc-pVTZ basis set).

the free energy profiles of Figure 4. In Table 3 we report the energy E_n of the protonation process

$$H_nF_n + H^+ \rightarrow H_{n+1}F_n^+$$

and the proton affinities A_n of an all-trans $(HF)_n$ chain computed in the gas phase at the MP2/6-311++G(d,p) and HCTH/PW levels of theory. The DFT calculations were performed as reported in section IIA. The inclusion of the thermal and the vibrational zero point energy contributions, in order to have the correct estimation of the proton affinity, decreases the values of the energy E_n by 15−25 kJ mol^{-1}. If we indicate with A_C the proton affinity for the process $CO+H^+ \rightarrow HCO^+$ and with A_O that for the process $CO+H^+ \rightarrow COH^+$, from Table 3 the following energy order can be inferred

$$A_O < A_1 < A_C < A_2 < A_3 < \cdots$$

The formation of HCO^+ is thermodynamically favorable with respect to H_2F^+ but not to $H_{n+1}F_n^+$ with $n > 1$. This means that the protonation of CO from H_2F^+ in the bulk solution, which is bonded to a more or less long HF chain, is an unfavorable process. In other words, from a thermodynamic point of view, the protonation of the CO molecule on the carbon side is feasible only if the proton comes from a one (maybe two) molecule chain. On the other hand, the formation of COH^+ is always unfavorable. Unfortunately, it is not possible to study the gas-phase reaction energies for the SbF_5–FH−$(FH)_{n-1}$ chains that would be more appropriate for a comparison with the trend observed in solution, since the system $SbF_5/(HF)_n$ has the tendency to form cyclic structures not present in the condensed phase (see SbF_5/HF (4% SbF_5).

B. Formyl Cation Reaction Channels. The formyl cation is extremely reactive. Once formed, it survives for a very short period of time (<1 ps). We have found two possible reactive channels for HCO^+. It can attack an $Sb_nF_{5n+1}^-$ anion to form H(F)CO, or it can transfer its proton to an F atom. In the following we will describe each of these two processes.

1. Formation of Formyl Fluoride, H(F)CO. The formyl cation can rapidly react with an Sb−F to yield H(F)CO. We have observed this reaction in both the 4% and 50% solutions. Immediately after its formation, H(F)CO gives rise to the weakly bonded complex H(O)CF→Sb_nF_{5n}, where the F atom is still coordinated to the Sb atom. The computed gas-phase formation energy is very small, e.g., −2.2 kJ mol^{-1} for $n = 1$ (Table 1), and the complex dissociates after few picoseconds. The time evolution of the Sb−F and C−F distances during the formation and the successive dissociation of the H(O)CF→SbF_5 complex in the 50% solution is shown in Figure 5a. We have not observed

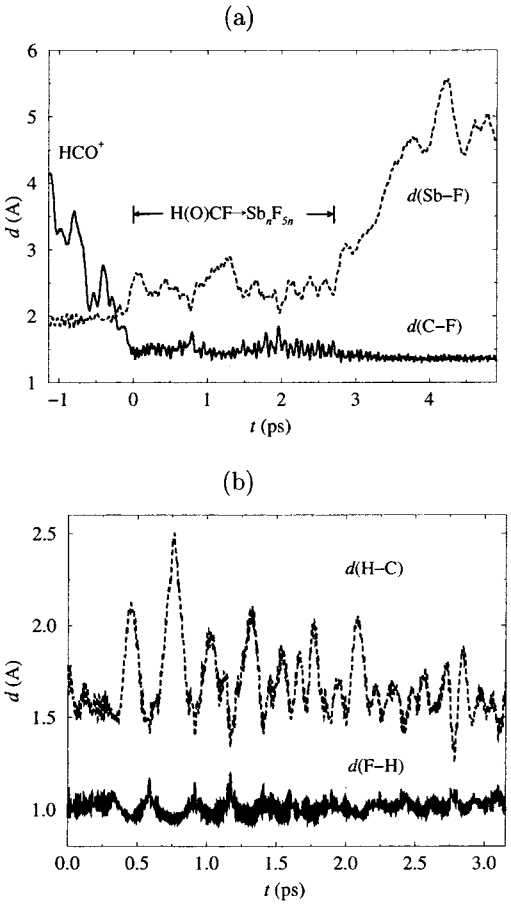

Figure 5. (a) Time evolution of the Sb−F (dashed) and C−F (solid) distances during the formation and the successive dissociation of the H(O)CF→SbF_5 complex. (b) Time evolution of the H−C (dashed) and F−H (solid) distances in the HF···CO complex.

the spontaneous formation of the H(F)CO→SbF_5 complex, which evidently happens on a longer time scale because of the slow reorientation time of the H(F)CO molecule. However, gas-phase calculations indicate that this complex is quite stable (formation energy of about −31 kJ mol^{-1}), and its formation, which would also restore the octahedral coordination of Sb, should be a very favorable process.

2. The Formyl Cation as Proton Carrier. The formyl cation can very easily donate its proton to a neighboring F atom. This process requires no barrier if the proton is transferred to an HF molecule belonging to an HF chain or a very low energy barrier if it is transferred to a F† atom of an SbF_6 unit. In the 50% solution, when HCO^+ approaches a F atom from the hydrogen side, it transfers the H^+ in agreement with the following mechanism:

$$\begin{aligned} X{-}F + HCO^+ &\rightleftharpoons X{-}F{\cdots}H{-}CO^+ \\ X{-}F \cdots H{-}CO^+ &\rightleftharpoons X{-}F{-}H^+{\cdots}CO \\ X{-}F{-}H^+{\cdots}CO &\rightleftharpoons X{-}F{-}H^+ + CO \end{aligned} \qquad (3)$$

where with X we have indicated the unit to which the F atom is bonded.

Although the X−F−H^+···CO complex is characterized by a large fluctuation of the H···C distance with an average value of about 1.6 Å, it seems to be quite stable, as can be seen from Figure 5b where the time evolution of the H−C and F−H distances in the complex are reported. However, from the constrained MD simulations we obtained an almost zero mean

TABLE 4: Carbonyl Vibrational Frequency (in cm^{-1}) in Different Environments

species	expt	this work
CO (gas)	2143[a]	2105[b]
CO (SbF_5/HF)		2130
HCO^+ (gas)	2184[c]	2168[b]
HCO^+ (SbF_5/HF)	2110[c]	(2020)
FH···CO (SbF_5/HF)		2050
H(F)CO→SbF_5 (gas)		1688
H(F)CO→SbF_5 (SbF_5/HF)	1671[c]	1725
H(O)CF→SbF_5 (SbF_5/HF)		1805

[a] Wilmer; et al. *Inorg. Chem.* **1990**, *120*, 2195; *J. Am. Chem. Soc.* **1992**, *114*, 8972. [b] Computed at 0 K by finite difference technique. [c] de Rege; et al. *Science* **1997**, *276*, 776.

force for the approach of HCO^+ to X−F. This means that the stabilization energy of the complex is of the order of statistical uncertainty of our calculations. The weakly bonded OC···HF complex has been known for a long time in the gas phase and also observed in the condensed phase by photodissociation of matrix-isolated formyl fluoride (see ref 65 and references therein).

Mechanism 3 is different from the one proposed by Olah et al.[11,12] that involves the COH^+ cation. Our gas-phase and solution calculations suggest that the formation of COH^+ cation is unlikely. First of all, the energy difference between formyl and isoformyl cations is too large (about 193 kJ mol^{-1} in gas phase, see also ref 66) to be involved in a fast (on the NMR time scale) exchange process. Moreover, as we have shown, the proton transfer to the oxygen atom is highly repulsive in solution and it does not lead to a stable state. Our calculations also show that the mechanism proposed by de Rege et al.[5] is not very likely. Besides the arguments just given about the isoformyl cation formation in solution, we have to keep in mind that gas-phase formation of the protoformyl dication, invoked by de Rege et al.,[5] requires a very high activation energy starting from both HCO^+ and COH^+cations (Table 1).

Mechanism 3 can also provide an explanation of the CO pressure (P_{CO}) dependence of the experimentally observed chemical shift and intensity of the HCO^+ ^{13}C NMR resonance relative to that of H(F)CO → SbF_5. As P_{CO} increases, the equilibria 3 predict an increase of HCO^+ or X−F···H−CO^+ concentration. Hence, the relative intensity of the NMR signals should be in favor of the formyl cation at higher pressure. Moreover, the H−$^{13}CO^+$ chemical shift should decrease as P_{CO} increases.

Other information supporting our conclusions is the trend of the C−O vibrational frequency ν(CO) during the reactive process. Experimentally a broad band at 2110 cm^{-1} is observed in the infrared spectrum. The band is assigned to HCO^+ somewhat modified by the presence of anionic species or SbF_5, or both, as the frequency red shift with respect to the gas value (2184 cm^{-1})[13,67] indicates. Table 4 reports our computed ν(CO) frequencies in several environments along with the experimental values. The frequency was calculated from the power spectrum of the autocorrelation function of the generalized velocity associated with the C−O stretching coordinate. Although the maximum entropy method has been used to obtain the power spectrum, the calculated frequencies have a large uncertainty (several tens of wavenumbers), due to the short length of the trajectories. However, the calculated values reproduce well the experimentally observed frequency downshift. Interestingly, the ν(CO) for the FH···CO complex is very close to that for HCO^+ in solution.

V. Conclusions

We have reported the results of a series ab initio CPMD simulations designed to probe the reactivity of CO in SbF_5/HF superacid media. The results obtained suggest that in dilute SbF_5/HF the acidity of H_2F^+ alone is not sufficient to protonate CO because of the strong H-bond interactions with the HF chain to which it is bonded. The formyl cation is favored only when the proton comes from a fluorine directly coordinated to an Sb atom. This situation is most likely, from a statistical point of view, in a 50% SbF_5−50% HF solution. Attempts to protonate CO on the oxygen side failed and no evidence of isoformyl cation or protoformyl cation was obtained. The experimentally observed fast proton exchange has been explained by invoking chemical equilibria in which the HCO^+ has a proton carrier role. We are aware that this interpretation could be oversimplified since solutions of SbF_5 in HF are know to involve complex equilibria between various $Sb_nF_{5n+1}^-$ anions,[62] whose formation may be inhibited by the small size of our simulation system. However, our model gives a vivid description of the first stages of HCO^+ chemistry in superacid solution. In particular, it already gives a reasonable explanation of many experimental findings.

Acknowledgment. We thank George A. Olah for stimulating our interest in this project. We send a special thanks to Mauro Boero and Dongsup Kim for helpful suggestions. The present study was supported by the National Science Fundation under Grant CHE-9623017. Some of the calculations were carried out at PSC with support provided by the Commonwealth of Pensylvania and the NSF NPACI program. Others used facilities supported in part by the NSF MRSEC program under Grant DMR009909.

References and Notes

(1) Zewail, A. H. *J. Phys. Chem. A* **2000**, *104*, 5660.
(2) Olah, G. A.; Prakash, G. K.; Sommers, J. *Superacids*; John Wiley and Sons: New York, 1985.
(3) Olah, G. A. *Angew. Chem., Int. Ed. Engl.* **1993**, *32*, 767.
(4) Pines, H. *The chemistry of catalytic hydrocarbons conversion*; Academic Press: New York, 1981.
(5) de Rege, P. J. F.; Gladysz, J. A.; Horváth, I. T. *Science* **1997**, *276*, 776.
(6) Buhl, D.; Snyder, L. E. *Nature* **1970**, *227*, 267.
(7) Klemperer, W. *Nature* **1970**, *227*, 1230.
(8) Warnatz, J. In *Combustion Chemistry*; Gardiner, J. W. C., Ed.; Springer-Verlag: Berlin, 1984.
(9) Harland, P. W.; Kim, N. D.; Petrie, S. A. H. *Aust. J. Chem.* **1989**, *2*, 9.
(10) Olah, G. A.; Dunne, K.; Mo, Y. L.; Szilahyi, P. *J. Am. Chem. Soc.* **1972**, *94*, 4200.
(11) Olah, G. A.; Laali, K.; Farooq, O. *J. Org. Chem.* **1985**, *50*, 1483.
(12) Prakash, G. K. *Science* **1997**, *276*, 756.
(13) Willner, H.; Aubke, F. *Inorg. Chem.* **1990**, *29*, 2195.
(14) Car, R.; Parrinello, M. *Phys. Rev. Lett.* **1985**, *55*, 2471.
(15) Kim, D.; Klein, M. L. *J. Am. Chem. Soc.* **1999**, *121*, 11251.
(16) Kim, D.; Klein, M. L. *Chem. Phys. Lett.* **1999**, *308*, 235.
(17) Kim, D.; Klein, M. L. *J. Phys. Chem. B* **2000**, *104*, 10074.
(18) Deng, L.; Branchadell, V.; Ziegler, T. *J. Am. Chem. Soc.* **1994**, *116*, 10645.
(19) Møller, C.; Plesset, M. *Phys. Rev.* **1934**, *46*, 618.
(20) Fan, L.; Ziegler, T. *J. Chem. Phys.* **1991**, *94*, 6057.
(21) Koch, W.; Holthausen, M. C. *A chemist's Guide to Density Functional Theory*; Wiley-VCH Verlag: Weinheim, 2000.
(22) Raugei, S.; Cardini, G.; Schettino, V. *J. Chem. Phys.* **1999**, *111*, 10887.
(23) Raugei, S.; Cardini, G.; Schettino, V. *J. Chem. Phys.* **2001**, *114*, 4089.
(24) Boero, M.; Parrinello, M.; Hüffer, S.; Weiss, H. *J. Am. Chem. Soc.* **2000**, *122*, 501.
(25) Boero, M.; Morikawa, Y.; Terakura, K.; Ozeki, M. *J. Chem. Phys.* **2000**, *112*, 9549.
(26) Mundy, C. J.; Hutter, J.; Parrinello, M. *J. Am. Chem. Soc.* **2000**, *122*, 4837.
(27) Mortensen, J. J.; Parrinello, M. *J. Phys. Chem. A* **2000**, *104*, 2901.

(28) Trout, B. L.; Parrinello, M. *J. Phys. Chem. B* **1999**, *103*, 6300.
(29) Frank, I.; Marx, D.; Parrinello, M. *J. Phys. Chem. A* **1999**, *103*, 7341.
(30) Hass, K. C.; Schneider, W. F.; Curioni, A.; Andreoni, W. *Science* **1997**, *119*, 265.
(31) Frank, I.; Parrinello, M.; Klamt, A. *J. Phys. Chem. A* **1998**, *102*, 3614.
(32) Meijer, E.; Sprik, M. *J. Am. Chem. Soc.* **1998**, *120*, 6345.
(33) Meijer, E.; Sprik, M. *J. Phys. Chem. A* **1998**, *102*, 2893.
(34) Doclo, K.; Röthlisberger, U. *Chem. Phys. Lett.* **1998**, *297*, 205.
(35) Aida, M.; Yamataka, H.; Dupuis, M. *Chem. Phys. Lett.* **1998**, *292*, 474.
(36) Bolton, K.; Hase, W.; Schlegel, H.; Song, K. *Chem. Phys. Lett.* **1998**, *288*, 621.
(37) Boero, M.; Parrinello, M.; Terakura, K. *J. Am. Chem. Soc.* **1998**, *120*, 2746.
(38) Curioni, A.; Sprik, M.; Andreoni, W.; Schiffer, H.; Hutter, J.; Parrinello, M. *J. Am. Chem. Soc.* **1997**, *119*, 7219.
(39) Backer, J.; Andzelm, J.; Muir, M.; Taylor, P. R. *Chem. Phys. Lett.* **1995**, *237*, 53.
(40) Parthiban, S.; de Oliveira, G.; Martin, J. M. L. *J. Phys. Chem. A* **2001**, *105*, 895.
(41) Becke, A. D. *Phys. Rev. A* **1998**, *38*, 3098.
(42) Lee, C.; Yang, W.; Parr, R. G. *Phys. Rev. B* **1988**, *37*, 785.
(43) Glukhovtsev, M. N.; Pross, A.; Radom, L. *J. Am. Chem. Soc.* **1995**, *117*, 2024.
(44) Glukhovtsev, M. N.; Bach, R.; Pross, A.; Radom, L. *Chem. Phys. Lett.* **1996**, *260*, 558.
(45) Hamprecht, F. A.; Cohen, A. J.; Tozer, D. J.; Handy, N. C. *J. Chem. Phys.* **1998**, *109*, 6264.
(46) Boese, A. D.; Doltsinis, N. L.; Handy, N. C.; Sprik, M. *J. Chem. Phys.* **2000**, *112*, 1670.
(47) Pagliai, M.; Raugei, S.; Cardini, G.; Schettino, V. *Phys. Chem. Chem. Phys.* **2001**, *3*, 2559.
(48) Troullier, N.; Martins, J. L. *Phys. Rev.* B **1991**, *43*, 1993.
(49) See, e.g.: Sprik, M.; Hutter, J.; Parrinello, M. *J. Chem. Phys.* **1996**, *105*, 1142; Giannozzi, P. In *Computational Approaches to Novel Condensed Matter Systems, Proceedings of 3rd Gordon Godfrey Workshop on Condensed Physics*; Neilson, D., Das M. P., Eds.; Plenum: New York, 1995.
(50) Kleinman, L.; Bylander, D. M. *Phys. Rev. Lett.* **1982**, *48*, 1425.
(51) Stich, I.; Car, R.; Parrinello, M.; Baroni, S. *Phys. Rev. B* **1989**, *39*, 4997.
(52) Hutter, J.; Alavi, A.; Deutsch, T.; Bernasconi, M.; Goedecker, S.; Marx, D.; Tuckerman, M.; Parrinello, M. *CPMD*; MPI für Festkörperforschung and IBM Zurich Research Laboratory, 1995−1999.
(53) Frisch, M. J.; Trucks, G. W.; Schlegel, H. B.; Scuseria, G. E.; Robb, M. A.; Cheeseman, J. R.; Zakrzewski, V. G.; Montgomery, J. A., Jr.; Stratmann, R. E.; Burant, J. C.; Dapprich, S.; Millam, J. M.; Daniels, A. D.; Kudin, K. N.; Strain, M. C.; Farkas, O.; Tomasi, J.; Barone, V.; Cossi, M.; Cammi, R.; Mennucci, B.; Pomelli, C.; Adamo, C.; Clifford, S.; Ochterski, J.; Petersson, G. A.; Ayala, P. Y.; Cui, Q.; Morokuma, K.; Malick, D. K.; Rabuck, A. D.; Raghavachari, K.; Foresman, J. B.; Cioslowski, J.; Ortiz, J. V.; Stefanov, B. B.; Liu, G.; Liashenko, A.; Piskorz, P.; Komaromi, I.; Gomperts, R.; Martin, R. L.; Fox, D. J.; Keith, T.; Al-Laham, M. A.; Peng, C. Y.; Nanayakkara, A.; Gonzalez, C.; Challacombe, M.; Gill, P. M. W.; Johnson, B. G.; Chen, W.; Wong, M. W.; Andres, J. L.; Head-Gordon, M.; Replogle, E. S.; Pople, J. A. *Gaussian 98*, revision A.5; Gaussian, Inc.: Pittsburgh, PA, 1998.
(54) Hockney, R. W. *Methods Comput. Phys.* **1970**, *9*, 136.
(55) Barnett, R. N.; Landman, U. *Phys. Rev. B* **1993**, *48*, 2081.
(56) Hartz, N.; Rasul, G.; Olah, G. A. *J. Am. Chem. Soc.* **1993**, *115*, 1277.
(57) Sprik, M.; Ciccotti, G. *J. Chem. Phys.* **1998**, *109*, 7737.
(58) Carter, E.; Ciccotti, G.; Hynes, J. T.; Kapral, R. *Chem. Phys. Lett.* **1989**, *98*, 472.
(59) Sprik, M. *Faraday Discuss.* **1998**, *110*, 437.
(60) Sprik, M. In *Rare Events and Dynamics of Classical and Quantum Condensed-Phase Systems—Classical and Quantum Dynamics in Condensed Phase Simulations*; Berne, B. J., Ciccotti, G., Coker, D. F., Eds.; World Scientific: Singapore, 1998; pp 285−309.
(61) Martyna, G. J.; Klein, M. L.; Tuckerman, M. E. *J. Chem. Phys.* **1992**, *97*, 2635.
(62) Donnell, T. A. *Superacids and acids melts as inorganic chemical reaction media*; VCH Publisher: New York, 1993.
(63) Gillespie, R. J.; Moss, K. C. *J. Chem. Soc. A* **1966**, *1966*, 1770.
(64) Geissler, P.; Dellago, C.; Chandler, D. *J. Phys. Chem. B* **1999**, *103*, 3706.
(65) Schatte, G.; Willner, H.; Hoge, D.; Knözinger, E.; Schrems, O. *J. Phys. Chem.* **1989**, *93*, 6025.
(66) Ma, N. L.; Smith, B. J.; Radom, L. *Chem. Phys. Lett.* **1992**, *197*, 573.
(67) Willner, H.; Aubke, F. *J. Am. Chem. Soc.* **1992**, *114*, 8972.